PROCEEDINGS OF SCIENCE

Extreme blazars: stacking analysis with KM3NeT/ARCA

M. R. Musone,[a,b,*] **A. Marinelli,**[a,c,d] **P. Migliozzi**[a] **and M. Petropoulou**[f,g] **on behalf of the KM3NeT Collaboration**

[a] *INFN - Sezione di Napoli, Complesso Univ. Monte S. Angelo, I-80126 Napoli, Italy*

[b] *Dipartimento di Fisica, Università degli studi della Campania Luigi Vanvitelli viale Lincoln 5, Caserta, 81100 Italy*

[c] *Dipartimento di Fisica "Ettore Pancini", Università degli studi di Napoli "Federico II", Complesso Univ. Monte S. Angelo, I-80126 Napoli, Italy*

[d] *INAF- Osservatorio Astronomico di Capodimonte, Salita Moiariello 16, I-80131, Napoli, Italy*

[f] *Department of Physics, National and Kapodistrian University of Athens, University Campus Zografos, GR 15784, Athens, Greece*

[g] *Institute of Accelerating Systems & Applications, University Campus Zografos, Athens, Greece*

E-mail: mrmusone@km3net.de

KM3NeT/ARCA is a large-scale underwater Cherenkov neutrino detector, currently under construction at the bottom of the Mediterranean Sea. The detector's geometry is optimised for the observation of TeV-PeV astrophysical neutrinos. Once completed, the detector will consist of 230 Detection Units (DUs). Each Detection Unit is an 800-meter vertical line that holds 18 Digital Optical Modules (DOMs), each containing 31 photomultiplier tubes. In this contribution we describe the analysis on Extreme High-frequency-peaked BL Lacs (EHBLs) blazars by integrating the theoretical modeling of these blazars, performed with the LeHaMoc numerical code, and in parallel the expectations of neutrinos emitted from these sources in binned likelihood stacking analyses based on KM3NeT/ARCA's data. We present a detailed analysis of a carefully selected sample of extreme blazars, focusing on their multiwavelength characteristics and high-energy emission mechanisms. This study represents a novel approach in the field, combining detailed modeling of the spectral energy distributions (SEDs) with a stacking sensitivity analysis tailored to this rare class of sources.

39th International Cosmic Ray Conference (ICRC2025)
15–24 July 2025
Geneva, Switzerland

ICRC 2025
The Astroparticle Physics Conference
Geneva July 15-24, 2025

*Speaker

https://pos.sissa.it/

PoS(ICRC2025)1125

1. Introduction

BL Lac objects are a subclass of blazars, i.e. active galactic nuclei (AGNs) whose relativistic jets are oriented toward the observer. They are the most abundant emitters of very high-energy (VHE) radiation in the extragalactic sky. Their spectral energy distribution (SED) is dominated by non-thermal radiation and typically exhibits two broad, distinct humps: one at low energy, attributed to synchrotron emission, and one at high energy, generally interpreted as inverse Compton (IC) scattering by relativistic electrons in the jet. BL Lac objects span a wide range of synchrotron peak frequencies, from infrared (IR) to X-ray regime, depending on the peak frequency νpeak in $\nu - \nu f_\nu$ space is higher than $10^{16.8}$ Hz, a blazar is usually called extreme high-energy synchrotron peaked (EHSP) [1] and are particularly relevant for high-energy astrophysics since they may be the counterparts of VHE γ-ray sources, high-energy astrophysical neutrinos, and ultra high-energy cosmic rays (UHECR). According the lepto-hadronic models EHBLs are interesting candidates for neutrino emission in the energy range of where the KM3NeT telescope is sensitive.The KM3NeT/ARCA is a new-generation of Cherenkov neutrino telescope under construction in the Mediterranean Sea [2]. It consists of a 3D grid of optical modules that detect the Cherenkov light from neutrino interaction products. The full detector will have 230 detection lines of 18 optical modules with a total effective volume of $\sim 1\ km^3$. Given its middle-latitude position, the detector will provide a complementary view of the sky with respect to IceCube. With KM3NeT/ARCA data taken with a partial configuration (6, 8, 19, and 21 detection units), the expected sensitivity of KM3NeT/ARCA to neutrino expectation from EHBLs sample are calculated using a stacking binned likelihood analysis. The methods and results are presented in this contribution.

2. EHBLs modeling

In this work we aim to perform a stacking analysis of EHBLs using numerical blazar SED models in order to increase the neutrino detection sensitivity with KM3NeT/ARCA detector. These models, which are calculated using the open-source code `LeHaMoC` [1] [4], take into account the relevant complex radiative processes responsible for neutrino production in blazar jets, providing precise predictions of the resulting neutrino spectra. We used the 3HSP catalog [3], the largest compilation of high-synchrotron-peaked blazars. It provides robust candidates that could be detected in X-ray surveys and provide promising targets for VHE/TeV observations and redshift estimates for 88% of the sources. It also provides key parameters related to the synchrotron peak for each source, including the peak frequency and the corresponding peak flux. Each source is assigned a Figure of Merit (FOM_x) reflecting its astrophysical relevance. The FOM_x is defined as the ratio of the flux at the synchrotron peak of a given source to the peak flux of the faintest 3HSP blazar in the TeV band. For this analysis, the selection of sources was based on the following criteria: a firm redshift estimation, a declination less than 40 degrees, a synchrotron peak frequency $\log_{10} \nu_{\rm pk}$ (Hz) > 16.8 and an available Fermi-LAT γ-ray counterpart. After these cuts were applied, the total number of EHBLs for this analysis is 88; Figure 1.

Out of the 88 EHBLs we chose three sources, namely 3HSPJ034923.2-115927, 3HSPJ023248.6+201717 and 3HSPJ235907.9-303740, to perform detailed SED fitting. These sources were selected for hav-

[1] `https://github.com/mariapetro/LeHaMoC/`

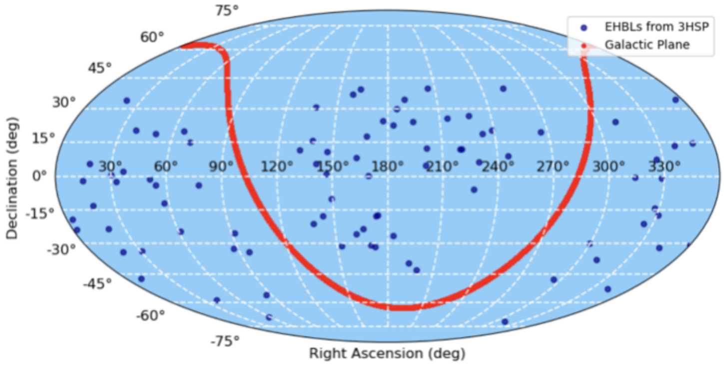

Figure 1: EHBLs skymap selected for stacking analysis from the 3HSP catalog.

ing an identical FOM_x while spanning a range of synchrotron peak frequencies. This makes them useful for scanning the behavior of the entire catalogue.. These results were later applied to the entire EHBL sample as described in Sect. 3.

2.1 Blazar model

The emitting region of the blazar jet is modeled as a spherical blob (in the jet comoving frame) with radius R that contains a tangled magnetic field of strength B; these are free parameters of the model. Because the emitting plasma moves with a bulk Lorentz factor $\Gamma \gg 1$ and is observed at a small angle θ (typically 2° - 5°), the emission is Doppler boosted. The Doppler factor, which is a free parameter of the model, is defined as $\delta = \Gamma^{-1}(1 - \beta\cos\theta)^{-1} \approx \Gamma$ for $\theta \sim 1/\Gamma$. Relativistic particles (primary electrons and protons) are injected into the blob at a constant rate with a broken power-law distribution. The slopes, minimum, maximum and break Lorentz factors of these distributions, as well as the associated energy injection rates, are model parameters to be determined by the fit. Charged particles will emit synchrotron photons that can be up-scattered to higher energies through inverse Compton scattering. Additionally, relativistic protons can produce secondary particles, such as electron-positron pairs and pions, through inelastic collisions with photons. Unstable secondary particles, such as pions and muons, eventually decay into pairs, gamma-rays, neutrinos, and anti-neutrinos. To quantify and track the time evolution of a stable particle species j in the blob, we solve a system of differential equations, also known as kinetic equations. For this, we used the open-source lepto-hadronic code `LeHaMoC`. The physical processes that are included in our calculations are: electron and proton synchrotron emission and absorption, inverse Compton scattering (for electrons only), $\gamma\gamma$ pair production, photopair (Bethe–Heitler) production, and photopion production processes.

Our main hypothesis is that the average SED of an extreme blazar is dominated by the emission of primary relativistic electrons, inspired by modeling results of TXS 0506+056 (e.g., [5]). Proton synchrotron radiation and any other associated secondary emission have subdominant contributions to the SED. Consequently, we fitted the SED with a leptonic model to constrain the primary electron distribution and source parameters (B, R, δ). Then, we added the hadronic component by setting the shape and characteristic Lorentz factors of the relativistic proton distribution equal to those of the injected electron distribution. We only left as a free parameter the ratio $\xi_{p/e} = L_p/L_e$, also

Table 1: Properties of extreme blazars used for SED modeling.

Name	Ra	Dec	Redshift	$\log(\nu_{\rm pk})$ (Hz)	FOM (X-rays)	FOM (γ-rays)
3HSPJ023248.6+20	38.20	+20.29	0.139	18.5	3.98	9.99
3HSPJ034923.2-11	57.35	-11.99	0.188	17.9	3.98	3.43
3HSPJ235907.9-30	359.78	-30.63	0.165	17.1	3.98	8.61

known as baryonic loading. Motivated by the recent modelling study of [6] (see e.g., Figure 10 therein), we adopted $\xi_{\rm p/e} = 10^4$ (see also [7]). For the leptonic fit we used the Markov Chain Monte Carlo (MCMC) sampler `emcee`. We used 32 parallel walkers on the prepared data for every source listed in Table 1. We varied the number of steps for each walker and concluded that 10,000 steps and a burn-in phase of 5,000 steps were sufficient for the model to converge and have a meaningful posterior sample. Our results are shown in Fig. 2.

3. Source selection results

We first defined the criteria guiding the selection of the three sources used for detailed SED modeling with the aim of extending this approach to the entire catalog. These sources have the same FOM_x value, but they differ in synchrotron peak frequency and γ-ray flux. Their redshift is in the range where we can find the majority of the sources in our sample (see Table 1).

Among the available data, X-ray observations are not always available, nor are the same instruments used, in contrast to Fermi-LAT data in γ-rays, which are available for all the selected sources. Therefore, using the integrated flux in the X-ray band as a scaling factor (or equivalently the FOM reported in the catalog) for the expected neutrino flux would not be reliable. Instead, we chose to use the integrated luminosity in the γ-ray band, specifically within the sensitivity range of the Fermi-LAT instrument (0.1-100 GeV). This approach allowed us to obtain a more consistent and homogeneous scaling factor across all sources, ensuring the application of uniform criteria. To this aim, for each modeled source, we evaluated the ratio between the integrated luminosity in the Fermi-LAT energy band and the value of the faintest source to define a new Figure of Merit for γ rays. The three selected sources rank among the top 10 in terms of $\mathrm{FOM_X}$ and among the top 20 in the FOM_γ [2]. In Fig. 2 we show the results of leptohadronic models performed with `LeHaMoC`.

3.1 Neutrino flux for stacking analysis

We approximate the neutrino emission of a blazar at redshift z_i from the EHBL sample by rescaling the neutrino flux spectrum obtained through the modeling of one of the three blazars in Table 1 (at redshift z_*). For this purpose, we also take into account the difference in γ-ray flux through FOM_γ:

$$F_{i,\nu} = F^*_\nu \left(\frac{1+z_i}{1+z_*}\right)^2 \left(\frac{L_{i,\gamma}}{L^*_\gamma}\right), \quad (1)$$

[2]is defined as ratio between integrate luminosity in FERMI energy range of each source with the same value of the faintest source in the catalogue.

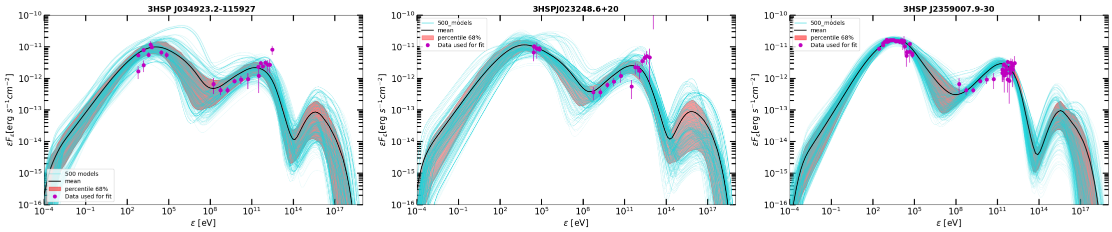

Figure 2: SEDs of the three EHBLs selected for modeling. Archival multi-wavelength observations from the SSDC SED Builder [8] are plotted with magenta markers. Thin colored lines show a representative sample of 500 model SEDs computed from the posterior distribution of the leptohadronic MCMC fit. The mean model SED is overplotted to guide the eye (black solid line).

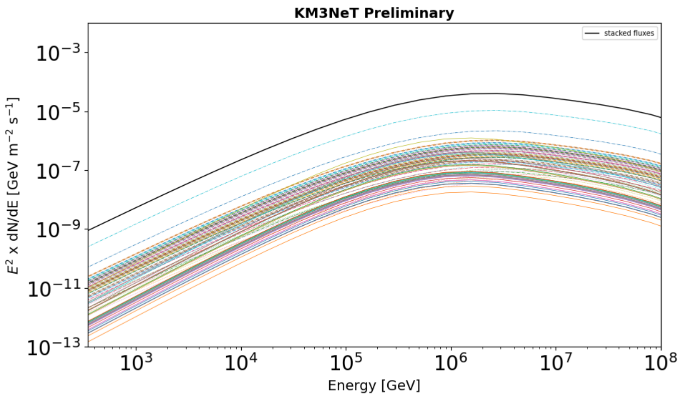

Figure 3: Expected neutrino fluxes for 88 EHBLs (colored lines) and their stacked flux (black line). Both neutrinos and antineutrinos population and their oscillated flavor composition at Earth are considered in the calculation.

where $F_\nu \equiv dN_\nu/d\varepsilon_\nu dt dA$ is the differential neutrino flux, and the energy of neutrinos is rescaled as

$$\frac{\varepsilon_{i,\nu}}{\varepsilon^*_\nu} = \frac{1+z_*}{1+z_i}. \tag{2}$$

To derive Eq. 1 we assumed that the ratio $Y = \frac{L_{i,\nu}}{L_{i,\gamma}}$ is fixed among sources; in particular, sources with $\log_{10}(\nu_{\rm pk})$ (Hz) < 17.1 have the same Y value as 3HSP J235907.9-30; sources with $\log_{10}(\nu_{\rm pk})$ (Hz) between 17.1 and 17.9 have the same Y value as 3HSP J034923.2-11 and sources with $\log_{10}(\nu_{\rm pk})$ (Hz) > 17.9 have the same Y value as 3HSPJ023248.6+20. We extended the analysis of whole catalogue under this strong assumption but we plan to model more sources in order to find a trend for the Y factor.The stacked neutrino flux from the sample of 88 EHBLs (using as reference sources listed in Table 1 is depicted in Fig. 3 as a black solid line, while colored dashed lines indicate the fluxes of individual blazars. The rescaling procedure introduces an uncertainty in the predicted neutrino flux, since it is based on a reference source and assumes that all other sources share the same Y factor. To account for the systematics introduced by our assumptions we introduce an uncertainty to the stacked neutrino flux. This is equal to the ratio between the expected neutrino flux for 3HSP J034923.2-11 obtained from the fit and the fluxes obtained by applying the rescaling method using the other two blazars as reference sources. This validation method was applied to all three blazars and the highest ratio value, in the energy range where 90% of the signal is expected for KM3NeT/ARCA6-21 for stacked fluxes, namely $\log_{10}\varepsilon_\nu$ 5.2 - 8 GeV energy range, was used to build the uncertainty band. In our analysis this value is 11.

4. Neutrino Data Sample

This analysis exploits different configurations of the ARCA detector, namely ARCA 6 (with a lifetime of 92 days), ARCA 8 (with a lifetime of 212.3 days), ARCA 19 (with a lifetime of 48.4 days), and ARCA 21 (with a lifetime of 287.4 days). Track-like events were used; these are mainly produced by charged-current interactions of muon neutrinos or tau neutrinos. Simulated events were produced using Monte Carlo generators as GSeaGen [10] and MUPAGE [11] respectively for neutrinos and muons. Subsequently, reconstruction algorithms were used to evaluate the direction and energy of the incoming neutrinos and muons. Several optimization cuts were made to reduce the amount of background produced by atmospheric muons and reject mis-reconstructed events. The event selection criteria follow those adopted for the point-source search developed with KM3NeT/ARCA6–21 [12]. Additional quality cuts using a boosted decision tree algorithm were adopted to reduce the contamination of mis-reconstructed muons in the sample.

5. Stacking analysis framework

This analysis relies on the binned likelihood method. The presence of signal emitted from point-like sources of neutrinos in the data is tested through 2D binned histograms. The variables of the histograms are the log_{10} of reconstructed neutrino energy($[10, 10^8]$ GeV) and the angular distance to the source ($[0, 5]°$). For the stacking analysis, each Region of Interest (RoI) is treated independently, and the total likelihood is defined as:

$$\mathcal{L} = \prod_{i,j} P(n_{ij}, \lambda\mu_s + \mu_b) \tag{3}$$

where $P(n, \mu)$ is the Poisson PDF for n observed data with an expected number of events, $\mu = \lambda \cdot \mu_s + \mu_b$. Here, μ_s is the expected signal events, μ_b the expected number of background events and λ is a free normalization of the signal. Pseudo experiments (PEs) are generated to evaluate the sensitivity of the detector. PEs are generated for a given "true" value of λ through randomly extracting a number for each bin following a Poisson distribution with an average value of $\lambda\mu_s^{i,j} + \mu_b^{i,j}$. For each PE, we perform a maximum likelihood ratio test, defining the Test Statistic (TS), which is given by

$$\mathrm{TS} = \log\left(\frac{\mathcal{L}(\tilde{\lambda})}{\mathcal{L}(0)}\right) \tag{4}$$

where $\tilde{\lambda}$ is the signal strength value maximising the likelihood for a given PE.

The sensitivity is defined using a frequentist approach based on pseudo-experiments (PEs) [9]. The model rejection factor (MRF) is defined as the signal strength value λ_{90} which satisfies

$$\int_{\mathrm{T_M}}^{+\infty} d(\mathrm{TS}|\lambda_{90})\mathrm{dTS} = 0.9 \tag{5}$$

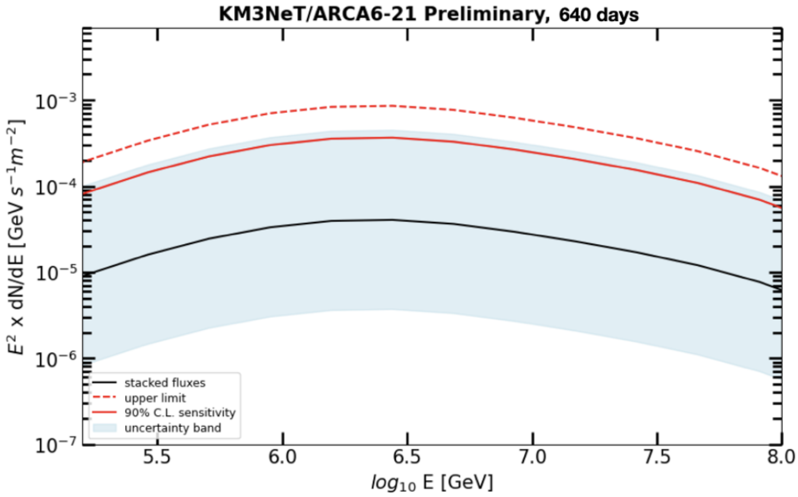

Figure 4: Sensitivity at 90% confidence level (solid black line) for the stacked flux (solid blue), shown in the energy range where 90% of the signal is expected. The shaded light-blue region indicates the flux uncertainty. The upper limit on the central flux is indicated as a red dashed line.

where T_M is the median TS of the background-only distribution.

The final sensitivity is

$$\phi_s(E) = \lambda_{90} \cdot \phi_{\text{input}}(E) \tag{6}$$

where ϕ_{input} is the input signal flux injected to evaluate the λ_{90} value.

5.1 Results

The sample was incrementally expanded by stacking catalogue sources, allowing the sensitivity enhancement to be studied as a function of source count. Beyond the first 40 sources, the incremental improvement became increasingly smaller until the catalogue was exhausted (totaling 88 sources). The sensitivity for the KM3NeT/ARCA6-21 dataset was determined over the energy range accounting for 90% of the expected signal; see Figure 4. The 90% confidence level sensitivity is approximately one order of magnitude above the stacked mean flux. The associated flux uncertainty described in Sec. 3.1 is also shown. After unblinding, no significant excess of events was observed over the background expectation. The calculated p-value is 4.6×10^{-3}, corresponding to a statistical significance of 2.6σ, in a one-tailed convention. The high significance is related to one single source 3HSP J204008.3-711459, which is one of the brightest sources in the catalogue. Then, 90% confidence level upper limits on the stacked flux have been derived and are shown in Figure 4.

6. Conclusion

In this work, we presented a stacking analysis, targeting extreme blazars selected from the 3HSP catalogue (88 EHBLs are included in our sample). The neutrino fluxes of extreme blazars were calculated using the code `LeHaMoC` and exploited data collected by KM3NeT/ARCA, with 6, 8, 19 and 21 DUs. The aim of a stacking analysis is to enhance the neutrino detection sensitivity, which may not be reached from individual sources alone. Although no significant excess has been observed, future improvements, such as increased exposure time and a larger effective area, will significantly boost ARCA's sensitivity and lead to better results. Overall, this analysis demonstrates a novel approach in the field, as it combines detailed modeling of the spectral energy distributions (SEDs) with a stacking sensitivity analysis for KM3NeT tailored to this rare class of sources.

Acknowledgements

MP acknowledges support from the Hellenic Foundation for Research and Innovation (H.F.R.I.) under the "2nd call for H.F.R.I. Research Projects to support Faculty members and Researchers" through the project UNTRAPHOB (Project ID 3013).

References

[1] Costamante L., Ghisellini G., and Giommi P., et al., A&A, 371(2), 512-526 .

[2] S. Adrian-Martinez et al., [KM3NeT Collaboration], 2016, J. Phys. G, Vol. 43, no. 8, 084001.

[3] Y. L. Chang et al., 2019, A&A, Vol.632, DOI: 10.1051/0004-6361/201834526

[4] S.I. Stathopoulos, M. Petropoulou, et al., A&A, 2019, Vol. 683, A225

[5] Keivani A., Murase K., Petropoulou M., Fox D. B., Cenko S. B., Chaty S., Coleiro A., et al., 2018, ApJ, 864, 84.

[6] X. Rodrigues, M. Karl, P. Padovani, P. Giommi, et al., A&A,2024, Vol. 689, A147, DOI: https://doi.org/10.1051/0004-6361/202450592.

[7] Petropoulou M., Oikonomou F., Mastichiadis A., Murase K., Padovani P., Vasilopoulos G., Giommi P., 2020, ApJ, 899, 113.

[8] Stratta G., Capalbi M., Giommi P., Primavera R., Cutini S. and Gasparrini, D., 2011, arXiv, 1103.0749.

[9] S. Aiello et al., [KM3NeT Collaboration] Astropart.Phys., 162:102990, 2024. DOI:10.1016/j.astropartphys.2024.102990

[10] S. Aiello *et al.* [KM3NeT Collaboration], Comput. Phys. Commun., 314:109660, 2025, Vol. 314 DOI:10.1016/j.cpc.2025.109660.

[11] G. Carminati, *et al.*, Comput. Phys. Commun.,2008, Vol. 179, 915–923. DOI: 10.1016/j.cpc.2008.07.014.

[12] V. Parisi *et al.*,[KM3NeT Collaboration] PoS **ICRC2025** (2025) 1124

Full Authors List: The KM3NeT Collaboration

O. Adriani 0000-0002-3592-0654[b,a], A. Albert[c,be], A. R. Alhebsi 0009-0002-7320-7638[d], S. Alshalloudi[d], M. Alshamsi[e], S. Alves Garre 0000-0003-1893-0858[f], F. Ameli[g], M. Andre[h], L. Aphecetche 0000-0001-7662-3878[i], M. Ardid 0000-0002-3199-594X[j], S. Ardid 0000-0003-4821-6655[j], J. Aublin[k], F. Badaracco 0000-0001-8553-7904[m,l], L. Bailly-Salins[n], B. Baret[k], A. Bariego-Quintana 0000-0001-5187-7505[f], M. Barnard 0000-0003-1720-7959[o], Y. Becherini[k], M. Bendahman[p], F. Benfenati Gualandi[r,q], M. Benhassi[s,p], D. M. Benoit 0000-0002-7773-6863[t], Z. Beňušová 0000-0002-2677-7657[v,u], E. Berbee[w], E. Berti[b], V. Bertin 0000-0001-6688-4580[e], P. Betti[b], S. Biagi 0000-0001-8598-0017[x], M. Boettcher[o], D. Bonanno 0000-0003-0223-3580[x], M. Bondì[y], S. Bottai[b], A. B. Bouasla[bf], J. Boumaaza[z], M. Bouta[e], M. Bouwhuis[w], C. Bozza 0000-0002-1797-6451[aa,p], R. M. Bozza[ab,p], H. Brânzaş[ac], F. Bretaudeau[i], M. Breuhaus 0000-0003-0268-5122[e], R. Bruijn[ad,w], J. Brunner[e], R. Bruno 0000-0002-3517-6597[y], E. Buis[w,ae], R. Buompane[s,p], I. Burriel[f], J. Busto[e], B. Caiffi[m], D. Calvo[f], A. Capone[g,af], F. Carenini[r,q], V. Carretero 0000-0002-7540-0266[ad,w], T. Cartraud[k], P. Castaldi[ag,q], V. Cecchini 0000-0003-4497-2584[f], S. Celli[g,af], L. Cerisy[e], M. Chabab[ah], A. Chen 0000-0001-6425-5692[ai], S. Cherubini[aj,x], T. Chiarusi[q], W. Chung[ak], M. Circella 0000-0002-5560-0762[al], R. Clark[am], R. Cocimano[x], J. A. B. Coelho[k], A. Coleiro[k], A. Condorelli[k], R. Coniglione[x], P. Coyle[e], A. Creusot[k], G. Cuttone[x], R. Dallier 0000-0001-9452-4849[i], A. De Benedittis[s,p], G. De Wasseige[am], V. Decoene[i], P. Deguire[e], I. Del Rosso[r,q], L. S. Di Mauro[x], I. Di Palma[g,af], A. F. Díaz[an], D. Diego-Tortosa 0000-0001-5546-3748[x], C. Distefano 0000-0001-8632-1136[x], A. Domi[ao], C. Donzaud[k], D. Dornic 0000-0001-5729-1468[e], E. Drakopoulou 0000-0003-2493-8039[ap], D. Drouhin 0000-0002-9719-2277[c,be], J.-G. Ducoin[e], P. Duverne[k], R. Dvornický 0000-0002-4401-1188[v], T. Eberl 0000-0002-5301-9106[ao], E. Eckerová[v,u], A. Eddymaoui[z], T. van Eeden[w], M. Eff[k], D. van Eijk[w], I. El Bojaddaini[aq], S. El Hedri[k], S. El Mentawi[e], V. Ellajosyula[m], A. Enzenhöfer[e], M. Farino[ak], G. Ferrara[aj,x], M. D. Filipović 0000-0002-4990-9288[ar], F. Filippini[q], D. Franciotti[x], L. A. Fusco[aa,p], T. Gal 0000-0001-7821-8673[ao], J. García Méndez 0000-0002-1580-0647[j], A. Garcia Soto 0000-0002-8186-2459[f], C. Gatius Oliver 0009-0002-1584-1788[w], N. Geißelbrecht[ao], E. Genton[am], H. Ghaddari[aq], L. Gialanella[s,p], B. K. Gibson[t], E. Giorgio[x], I. Goos 0009-0008-1479-539X[k], P. Goswami[k], S. R. Gozzini 0000-0001-5152-9631[f], R. Gracia[ao], B. Guillon[n], C. Haack[ao], C. Hanna[ak], H. van Haren[as], E. Hazelton[ak], A. Heijboer[w], L. Hennig[ao], J. J. Hernández-Rey[f], A. Idrissi 0000-0001-8936-6364[x], W. Idrissi Ibnsalih[p], G. Illuminati[q], R. Jaimes[f], O. Janik[ao], D. Joly[e], M. de Jong[at,w], P. de Jong[ad,w], B. J. Jung[w], P. Kalaczyński 0000-0001-9278-5906[bg,au], U. F. Katz[ao], J. Keegans[t], V. Kikvadze[av], G. Kistauri[aw,av], C. Kopper 0000-0001-6288-7637[ao], A. Kouchner[ax,k], Y. Y. Kovalev 0000-0001-9303-3263[ay], L. Krupa[u], V. Kueviakoe[w], V. Kulikovskiy[m], R. Kvatadze[aw], M. Labalme[n], R. Lahmann[ao], M. Lamoureux 0000-0002-8860-5826[am], A. Langella 0000-0001-6273-3558[ak], G. Larosa[x], C. Lastoria[n], J. Lazar[am], A. Lazo[f], G. Lehaut[n], V. Lemaître[am], E. Leonora[y], N. Lessing[f], G. Levi[r,q], M. Lindsey Clark[k], F. Longhitano[y], S. Madarapu[f], F. Magnani[e], L. Malerba[m,l], F. Mamedov[u], A. Manfreda 0000-0002-0998-4953[p], A. Manousakis[az], M. Marconi 0009-0008-0023-4647[l,m], A. Margiotta 0000-0001-6929-5386[r,q], A. Marinelli[ab,p], C. Markou[ap], L. Martin 0000-0002-9781-2632[i], M. Mastrodicasa[af,g], S. Mastroianni[p], J. Mauro 0009-0005-9324-7970[am], K. C. K. Mehta[au], G. Miele[ab,p], P. Migliozzi 0000-0001-5497-3594[p], E. Migneco[x], M. L. Mitsou[s,p], C. M. Mollo[p], L. Morales-Gallegos 0000-0002-2241-4365[s,p], N. Mori 0000-0003-2138-3787[b], A. Moussa 0000-0003-2233-9120[aq], I. Mozun Mateo[n], R. Muller 0000-0002-5247-7084[q], M. R. Musone[s,p], M. Musumeci[x], S. Navas 0000-0003-1688-5758[ba], A. Nayerhoda[al], C. A. Nicolau[g], B. Nkosi 0000-0003-0954-4779[ai], B. Ó Fearraigh 0000-0002-1795-1617[m], V. Oliviero 0009-0004-9638-0825[ab,p], A. Orlando[x], E. Oukacha[k], L. Pacini 0000-0001-6808-9396[b], D. Paesani[x], J. Palacios González 0000-0001-9292-9981[f], G. Papalashvili[al,av], P. Papini[b], V. Parisi[l,m], A. Parmar[n], C. Pastore[al], A. M. Păun[ac], G. E. Păvălaş[ac], S. Peña Martínez 0000-0001-8939-0639[k], M. Perrin-Terrin[e], V. Pestel[n], M. Petropavlova 0000-0002-0416-0795[u,bh], P. Piattelli[x], A. Plavin[ay,bi], C. Poirè[aa,p], V. Popa[†2ac], T. Pradier 0000-0001-5501-0060[c], J. Prado[f], S. Pulvirenti[x], C.A. Quiroz-Rangel 0009-0002-3446-8747[j], N. Randazzo[y], A. Ratnani[bb], S. Razzaque[bc], I. C. Rea 0000-0002-3954-7754[p], D. Real 0000-0002-1038-7021[f], G. Riccobene 0000-0002-0600-2774[x], J. Robinson[o], A. Romanov[l,m,n], E. Ros[ay], A. Šaina[f], F. Salesa Greus 0000-0002-8610-8703[f], D. F. E. Samtleben[at,w], A. Sánchez Losa 0000-0001-9596-7078[f], S. Sanfilippo[x], M. Sanguineti[l,m], D. Santonocito[x], P. Sapienza[x], M. Scaringella[b], M. Scarnera[am,k], J. Schnabel[ao], J. Schumann 0000-0003-3722-086X[ao], J. Seneca[w], P. A. Sevle Myhr 0009-0005-9103-4410[am], I. Sgura[al], R. Shanidze[av], Chengyu Shao 0000-0002-2954-1180[bj,e], A. Sharma[k], Y. Shitov[u], F. Šimkovic[v], A. Simonelli[p], A. Sinopoulou 0000-0001-9205-8813[y], B. Spisso[p], M. Spurio 0000-0002-8698-3655[r,q], O. Starodubtsev[b], D. Stavropoulos[ap], I. Štekl[u], D. Stocco 0000-0002-5377-5163[i], M. Taiuti[l,m], Y. Tayalati[z,bb], H. Thiersen[o], I. Tosta e Melo[y,aj], B. Trocmé 0000-0001-9500-2487[k], V. Tsourapis 0009-0000-5616-5662[ap], C. Tully 0000-0001-6771-2174[ak], E. Tzamariudaki[ap], A. Ukleja 0000-0003-0480-4850[au], A. Vacheret[n], V. Valsecchi[x], V. Van Elewyck[ax,k], G. Vannoye[l,m], E. Vannuccini[b], G. Vasileiadis[bd], F. Vazquez de Sola[w], A. Veutro[g,af], S. Viola[x], D. Vivolo[s,p], A. van Vliet 0000-0003-2827-3361[d], E. de Wolf 0000-0002-8272-8681[ad,w], I. Lhenry-Yvon[k], S. Zavatarelli[m], D. Zito[x], J. D. Zornoza 0000-0002-1834-0690[f], and J. Zúñiga 0000-0002-1041-6451[f].

[a]Università di Firenze, Dipartimento di Fisica e Astronomia, via Sansone 1, Sesto Fiorentino, 50019 Italy
[b]INFN, Sezione di Firenze, via Sansone 1, Sesto Fiorentino, 50019 Italy
[c]Université de Strasbourg, CNRS, IPHC UMR 7178, F-67000 Strasbourg, France
[d]Khalifa University of Science and Technology, Department of Physics, PO Box 127788, Abu Dhabi, United Arab Emirates
[e]Aix Marseille Univ, CNRS/IN2P3, CPPM, Marseille, France
[f]IFIC - Instituto de Física Corpuscular (CSIC - Universitat de València), c/Catedrático José Beltrán, 2, 46980 Paterna, Valencia, Spain
[g]INFN, Sezione di Roma, Piazzale Aldo Moro, 2 - c/o Dipartimento di Fisica, Edificio, G.Marconi, Roma, 00185 Italy
[h]Universitat Politècnica de Catalunya, Laboratori d'Aplicacions Bioacústiques, Centre Tecnològic de Vilanova i la Geltrú, Avda. Ram-

[2]Deceased

bla Exposició, s/n, Vilanova i la Geltrú, 08800 Spain
[i]Subatech, IMT Atlantique, IN2P3-CNRS, Nantes Université, 4 rue Alfred Kastler - La Chantrerie, Nantes, BP 20722 44307 France
[j]Universitat Politècnica de València, Instituto de Investigación para la Gestión Integrada de las Zonas Costeras, C/ Paranimf, 1, Gandia, 46730 Spain
[k]Université Paris Cité, CNRS, Astroparticule et Cosmologie, F-75013 Paris, France
[l]Università di Genova, Via Dodecaneso 33, Genova, 16146 Italy
[m]INFN, Sezione di Genova, Via Dodecaneso 33, Genova, 16146 Italy
[n]LPC CAEN, Normandie Univ, ENSICAEN, UNICAEN, CNRS/IN2P3, 6 boulevard Maréchal Juin, Caen, 14050 France
[o]North-West University, Centre for Space Research, Private Bag X6001, Potchefstroom, 2520 South Africa
[p]INFN, Sezione di Napoli, Complesso Universitario di Monte S. Angelo, Via Cintia ed. G, Napoli, 80126 Italy
[q]INFN, Sezione di Bologna, v.le C. Berti-Pichat, 6/2, Bologna, 40127 Italy
[r]Università di Bologna, Dipartimento di Fisica e Astronomia, v.le C. Berti-Pichat, 6/2, Bologna, 40127 Italy
[s]Università degli Studi della Campania "Luigi Vanvitelli", Dipartimento di Matematica e Fisica, viale Lincoln 5, Caserta, 81100 Italy
[t]E. A. Milne Centre for Astrophysics, University of Hull, Hull, HU6 7RX, United Kingdom
[u]Czech Technical University in Prague, Institute of Experimental and Applied Physics, Husova 240/5, Prague, 110 00 Czech Republic
[v]Comenius University in Bratislava, Department of Nuclear Physics and Biophysics, Mlynska dolina F1, Bratislava, 842 48 Slovak Republic
[w]Nikhef, National Institute for Subatomic Physics, PO Box 41882, Amsterdam, 1009 DB Netherlands
[x]INFN, Laboratori Nazionali del Sud, (LNS) Via S. Sofia 62, Catania, 95123 Italy
[y]INFN, Sezione di Catania, (INFN-CT) Via Santa Sofia 64, Catania, 95123 Italy
[z]University Mohammed V in Rabat, Faculty of Sciences, 4 av. Ibn Battouta, B.P. 1014, R.P. 10000 Rabat, Morocco
[aa]Università di Salerno e INFN Gruppo Collegato di Salerno, Dipartimento di Fisica, Via Giovanni Paolo II 132, Fisciano, 84084 Italy
[ab]Università di Napoli “Federico II”, Dip. Scienze Fisiche “E. Pancini”, Complesso Universitario di Monte S. Angelo, Via Cintia ed. G, Napoli, 80126 Italy
[ac]Institute of Space Science - INFLPR Subsidiary, 409 Atomistilor Street, Magurele, Ilfov, 077125 Romania
[ad]University of Amsterdam, Institute of Physics/IHEF, PO Box 94216, Amsterdam, 1090 GE Netherlands
[ae]TNO, Technical Sciences, PO Box 155, Delft, 2600 AD Netherlands
[af]Università La Sapienza, Dipartimento di Fisica, Piazzale Aldo Moro 2, Roma, 00185 Italy
[ag]Università di Bologna, Dipartimento di Ingegneria dell’Energia Elettrica e dell’Informazione "Guglielmo Marconi", Via dell’Università 50, Cesena, 47521 Italia
[ah]Cadi Ayyad University, Physics Department, Faculty of Science Semlalia, Av. My Abdellah, P.O.B. 2390, Marrakech, 40000 Morocco
[ai]University of the Witwatersrand, School of Physics, Private Bag 3, Johannesburg, Wits 2050 South Africa
[aj]Università di Catania, Dipartimento di Fisica e Astronomia "Ettore Majorana", (INFN-CT) Via Santa Sofia 64, Catania, 95123 Italy
[ak]Princeton University, Department of Physics, Jadwin Hall, Princeton, New Jersey, 08544 USA
[al]INFN, Sezione di Bari, via Orabona, 4, Bari, 70125 Italy
[am]UCLouvain, Centre for Cosmology, Particle Physics and Phenomenology, Chemin du Cyclotron, 2, Louvain-la-Neuve, 1348 Belgium
[an]University of Granada, Department of Computer Engineering, Automation and Robotics / CITIC, 18071 Granada, Spain
[ao]Friedrich-Alexander-Universität Erlangen-Nürnberg (FAU), Erlangen Centre for Astroparticle Physics, Nikolaus-Fiebiger-Straße 2, 91058 Erlangen, Germany
[ap]NCSR Demokritos, Institute of Nuclear and Particle Physics, Ag. Paraskevi Attikis, Athens, 15310 Greece
[aq]University Mohammed I, Faculty of Sciences, BV Mohammed VI, B.P. 717, R.P. 60000 Oujda, Morocco
[ar]Western Sydney University, School of Science, Locked Bag 1797, Penrith, NSW 2751 Australia
[as]NIOZ (Royal Netherlands Institute for Sea Research), PO Box 59, Den Burg, Texel, 1790 AB, the Netherlands
[at]Leiden University, Leiden Institute of Physics, PO Box 9504, Leiden, 2300 RA Netherlands
[au]AGH University of Krakow, Al. Mickiewicza 30, 30-059 Krakow, Poland
[av]Tbilisi State University, Department of Physics, 3, Chavchavadze Ave., Tbilisi, 0179 Georgia
[aw]The University of Georgia, Institute of Physics, Kostava str. 77, Tbilisi, 0171 Georgia
[ax]Institut Universitaire de France, 1 rue Descartes, Paris, 75005 France
[ay]Max-Planck-Institut für Radioastronomie, Auf dem Hügel 69, 53121 Bonn, Germany
[az]University of Sharjah, Sharjah Academy for Astronomy, Space Sciences, and Technology, University Campus - POB 27272, Sharjah, - United Arab Emirates
[ba]University of Granada, Dpto. de Física Teórica y del Cosmos & C.A.F.P.E., 18071 Granada, Spain
[bb]School of Applied and Engineering Physics, Mohammed VI Polytechnic University, Ben Guerir, 43150, Morocco
[bc]University of Johannesburg, Department Physics, PO Box 524, Auckland Park, 2006 South Africa
[bd]Laboratoire Univers et Particules de Montpellier, Place Eugène Bataillon - CC 72, Montpellier Cédex 05, 34095 France
[be]Université de Haute Alsace, rue des Frères Lumière, 68093 Mulhouse Cedex, France
[bf]Université Badji Mokhtar, Département de Physique, Faculté des Sciences, Laboratoire de Physique des Rayonnements, B. P. 12, Annaba, 23000 Algeria
[bg]AstroCeNT, Nicolaus Copernicus Astronomical Center, Polish Academy of Sciences, Rektorska 4, Warsaw, 00-614 Poland
[bh]Charles University, Faculty of Mathematics and Physics, Ovocný trh 5, Prague, 116 36 Czech Republic
[bi]Harvard University, Black Hole Initiative, 20 Garden Street, Cambridge, MA 02138 USA

PoS(ICRC2025)1125

Acknowledgements

The authors acknowledge the financial support of: KM3NeT-INFRADEV2 project, funded by the European Union Horizon Europe Research and Innovation Programme under grant agreement No 101079679; Funds for Scientific Research (FRS-FNRS), Francqui foundation, BAEF foundation. Czech Science Foundation (GAČR 24-12702S); Agence Nationale de la Recherche (contract ANR-15-CE31-0020), Centre National de la Recherche Scientifique (CNRS), Commission Européenne (FEDER fund and Marie Curie Program), LabEx UnivEarthS (ANR-10-LABX-0023 and ANR-18-IDEX-0001), Paris Île-de-France Region, Normandy Region (Alpha, Blue-waves and Neptune), France, The Provence-Alpes-Côte d'Azur Delegation for Research and Innovation (DRARI), the Provence-Alpes-Côte d'Azur region, the Bouches-du-Rhône Departmental Council, the Metropolis of Aix-Marseille Provence and the City of Marseille through the CPER 2021-2027 NEUMED project, The CNRS Institut National de Physique Nucléaire et de Physique des Particules (IN2P3); Shota Rustaveli National Science Foundation of Georgia (SRNSFG, FR-22-13708), Georgia; This research was funded by the European Union (ERC MuSES project No 101142396); The General Secretariat of Research and Innovation (GSRI), Greece; Istituto Nazionale di Fisica Nucleare (INFN) and Ministero dell'Università e della Ricerca (MUR), through PRIN 2022 program (Grant PANTHEON 2022E2J4RK, Next Generation EU) and PON R&I program (Avviso n. 424 del 28 febbraio 2018, Progetto PACK-PIR01 00021), Italy; IDMAR project Po-Fesr Sicilian Region az. 1.5.1; A. De Benedittis, W. Idrissi Ibnsalih, M. Bendahman, A. Nayerhoda, G. Papalashvili, I. C. Rea, A. Simonelli have been supported by the Italian Ministero dell'Università e della Ricerca (MUR), Progetto CIR01 00021 (Avviso n. 2595 del 24 dicembre 2019); KM3NeT4RR MUR Project National Recovery and Resilience Plan (NRRP), Mission 4 Component 2 Investment 3.1, Funded by the European Union – NextGenerationEU,CUP I57G21000040001, Concession Decree MUR No. n. Prot. 123 del 21/06/2022; Ministry of Higher Education, Scientific Research and Innovation, Morocco, and the Arab Fund for Economic and Social Development, Kuwait; Nederlandse organisatie voor Wetenschappelijk Onderzoek (NWO), the Netherlands; The grant "AstroCeNT: Particle Astrophysics Science and Technology Centre", carried out within the International Research Agendas programme of the Foundation for Polish Science financed by the European Union under the European Regional Development Fund; The program: "Excellence initiative-research university" for the AGH University in Krakow; The ARTIQ project: UMO-2021/01/2/ST6/00004 and ARTIQ/0004/2021; Ministry of Education and Scientific Research, Romania; Slovak Research and Development Agency under Contract No. APVV-22-0413; Ministry of Education, Research, Development and Youth of the Slovak Republic; MCIN for PID2021-124591NB-C41, -C42, -C43 and PDC2023-145913-I00 funded by MCIN/AEI/10.13039/501100011033 and by "ERDF A way of making Europe", for ASFAE/2022/014 and ASFAE/2022 /023 with funding from the EU NextGenerationEU (PRTR-C17.I01) and Generalitat Valenciana, for Grant AST22_6.2 with funding from Consejería de Universidad, Investigación e Innovación and Gobierno de España and European Union - NextGenerationEU, for CSIC-INFRA23013 and for CNS2023-144099, Generalitat Valenciana for CIDEGENT/2020/049, CIDEGENT/2021/23, CIDEIG/2023/20, ESGENT2024/24, CIPROM/2023/51, GRISOLIAP/2021/192 and INNVA1/2024/110 (IVACE+i), Spain; Khalifa University internal grants (ESIG-2023-008, RIG-2023-070 and RIG-2024-047), United Arab Emirates; The European Union's Horizon 2020 Research and Innovation Programme (ChETEC-INFRA - Project no. 101008324).

Views and opinions expressed are those of the author(s) only and do not necessarily reflect those of the European Union or the European Research Council. Neither the European Union nor the granting authority can be held responsible for them.